Rare Events Detected with a Bulk Acoustic Wave High Frequency Gravitational Wave Antenna

Maxim Goryachev,[1] William M. Campbell,[1] Ik Siong Heng,[2] Serge Galliou,[3] Eugene N. Ivanov,[1] and Michael E. Tobar[1,*]

[1]*ARC Centre of Excellence for Engineered Quantum Systems, ARC Centre of Excellence for Dark Matter Particle Physics, Department of Physics, University of Western Australia, 35 Stirling Highway, Crawley, Western Australia 6009, Australia*
[2]*SUPA, School of Physics and Astronomy, University of Glasgow, Glasgow, Scotland G12 8QQ, United Kingdom*
[3]*Department of Time and Frequency, FEMTO-ST Institute, ENSMM, 26 Chemin de l'Épitaphe, 25000 Besançon, France*

(Received 12 February 2021; revised 7 April 2021; accepted 16 July 2021; published 12 August 2021)

This work describes the operation of a high frequency gravitational wave detector based on a cryogenic bulk acoustic wave cavity and reports observation of rare events during 153 days of operation over two separate experimental runs (run 1 and run 2). In both run 1 and run 2, two modes were simultaneously monitored. Across both runs, the third overtone of the fast shear mode (3B) operating at 5.506 MHz was monitored; whereas in run 1, the second mode was chosen to be the fifth overtone of the slow shear mode (5C) operating at 8.392 MHz. However, in run 2, the second mode was selected to be closer in frequency to the first mode; and it was chosen to be the third overtone of the slow shear mode (3C) operating at 4.993 MHz. Two strong events were observed as transients responding to energy deposition within acoustic modes of the cavity. The first event occurred during run 1 on 12 May 2019 (UTC), and it was observed in the 5.506 MHz mode; whereas the second mode at 8.392 MHz observed no event. During run 2, a second event occurred on 27 November 2019 (UTC) and was observed by both modes. Timings of the events were checked against available environmental observations as well as data from other detectors. Various possibilities explaining the origins of the events are discussed.

DOI: 10.1103/PhysRevLett.127.071102

Introduction.—Gravitational wave (GW) astronomy became a reality on 14 September 2015 [1]. Since then, GW interferometric detectors have provided additional channels for studying the Universe and have complemented observations conducted with telescopes. However, current operating GW interferometric detectors are only capable of probing spacetime in a relatively narrow band of frequency (100 Hz–1 kHz), unlike the electromagnetic spectrum, where observations may be conducted over a vast frequency range (from low radio frequency to x ray). Recently, high frequency gravitational waves (HFGWs) have been considered as probes for new physics, as outlined in the recent white paper on this topic [2]; thus, the need for GW detectors with higher frequency capabilities is well motivated and has been considered in a significant way by the community [3–12]. In this work, we present the first fast signal analysis of a HFGW detector based on a high frequency acoustic cavity, with plans of further analysis of slow signals and fluctuations to follow in a subsequent work.

The HFGW detector employed in this work was proposed in 2014 [13]; it is based on the principles of the resonant-mass GW detector, which were operational from the 1990s, mainly as resonant bars or spheres [14–20]. Besides our detector, different variants of the macroscopic resonant-mass detector have been recently proposed to detect HFGWs [21,22]. In the current form, our system is based on extremely high quality factor quartz bulk acoustic wave (BAW) cavities [23,24] and a superconducting quantum interference device (SQUID) amplifier operating at 3.4 K in a closed cycle cryocooler, with a schematic shown in Fig 1. This detector is essentially a multimode resonant-mass GW antenna working on different overtones

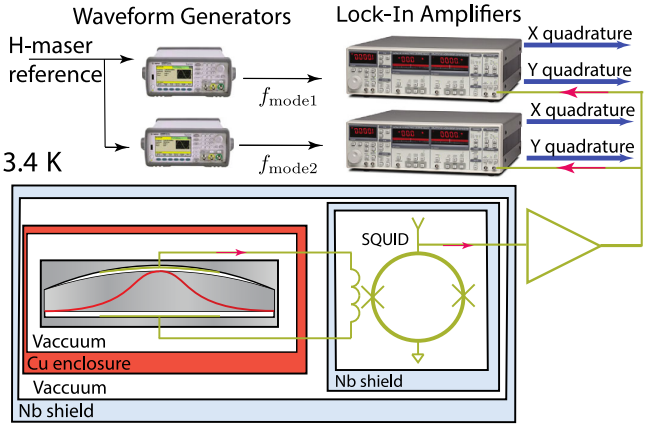

FIG. 1. Experimental setup showing BAW cavity connected to SQUID amplifier and shielding arrangement. Note that 4 and 50 K shields as well as stainless still vacuum chamber not shown.

(OTs) of its acoustic modes that are sensitive to GWs. The high quality of these modes (reaching 4×10^9 for high OT modes [23]) has been achieved by employing energy trapping technology of the quartz crystal plate. Due to the piezoelectric properties of quartz crystals, the system's acoustic modes that display sensitivity to GW strains can be read out via piezoelectric coupling to capacitive electrodes held at small gaps from the vibrating body. Three different acoustic mode families in the bulk of the device can be observed with this setup: longitudinal phonon or A modes, quasifast shear or B modes, and quasislow shear or C modes. The shear wave splitting arises from anisotropies in the crystal creating different phonon speeds, depending on the wave's polarization. The resonating device is composed of an approximately 1 mm thick plano-covex BVA SC-cut [25–27] quartz plate that is 30 mm in diameter, and it is situated in a copper enclosure with only two isolated signal pins protruding [28]. This enclosure is placed under a dedicated vacuum held at pressures lower than 10^{-6} mbar, and it is isolated from the vacuum of the cryocooler chamber. The readout electrodes are inductively coupled to a Magnicon SQUID sensor with input inductance of 400 nH that, when appropriately biased, provides linear amplification and effective current-to-voltage transduction characterized by a transimpedance of 1.2 MΩ. This readout system allows for an extremely low noise floor set by the magnetic flux noise of the SQUID, which was inferred from the output voltage noise floor to be $\approx 1.1 \mu\phi_0/\sqrt{\text{Hz}}$ at 5.506 MHz, where ϕ_0 is the flux quantum. The setup has been demonstrated previously, which confirmed the low noise operation limited only by the fundamental Nyquist thermal fluctuations due to ambient temperature, and combined with the intrinsic SQUID amplifier readout noise [29]. To improve thermal and electrical isolation, both the quartz BAW cavity and the SQUID were contained in a large niobium shield, which was also used to support the structure. The whole setup was also covered by 4 and 50 K antiradiation shields as well as a vacuum chamber ensuring the pressure of $\sim 3 \times 10^{-6}$ mbar. The output of the SQUID system was further amplified at room temperature, and the signal was split between two stand-alone SRS SR844 lock-in amplifiers. Each of these lock-in amplifiers was tuned close to a particular resonance frequency of the BAW cavity to down-convert its signal close to direct current. The corresponding frequency reference signals were produced by commercial waveform signal generators locked to a hydrogen maser. In this arrangement, each lock-in amplifier produced two quadratures of a signal, giving four available output channels in total. The resulting signals were digitized using a multichannel acquisition system with the sampling rate of 100 Hz. The setup was located in a basement laboratory in Perth, Western Australia (31.98 °S, 115.819 °E).

The timeline of the HFGW search is shown in Fig. 2. The operation was split between two runs due to a data

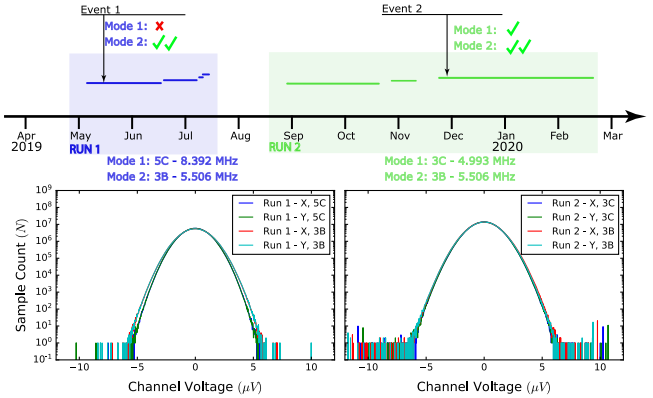

FIG. 2. Timeline of described experiment as well as histogram of total data collection at the detector output. Blue and green lines on timeline show separate data acquisition periods for two runs. Arrows point to the dates of two observed events.

acquisition system upgrade; the first observational run saw 1616.7 h of active operation at a duty rate of 98.27%, with the following run active for 4055.6 h at a rate of 91.89%. During the first run, the fifth OT of the slow shear mode at 8.392 MHz (5B) and the third OT of the fast shear mode at 5.506 MHz (3B) of the BAW cavity were continuously monitored. For the second run, the third OT of the slow shear mode at 4.993 MHz (3C) and the 3B mode were monitored. The modes available for monitoring at this stage of the experiment were limited by the SQUID electronics having a 3 dB bandwidth of only 2.1 MHz. This limited our choice of overtone modes to those under 20.4 MHz, with typical quality factors in the tens of millions. This is a minor technical obstacle that will be overcome with future upgrades to the setup, allowing for higher OT modes with better quality factors to be monitored. For the 3B, 3C, and 5C modes, the quality factors were previously reported to be 44, 48, and 10.7 million, respectively, as detailed in Ref. [29]. For consistency, we estimated the quality factor by fitting to the power spectrum of the current datasets; this showed close agreement to the previously reported values.

Figure 3 presents the amplitude spectral densities of both quadratures demodulated near two resonance frequencies for the longest continuous data acquisition (2227.8 h). All signals demonstrate clear Lorentzian peaks corresponding to thermal (Nyquist) noise of the acoustic modes of the BAW device [29], whereas broadband features are set by the flux noise floor of the SQUID. We have also included the spectral strain sensitivity of the device, which can be calculated from the corresponding voltage power spectral densities at the SQUID output using the transfer function

$$H(i\omega) = \frac{\kappa_\lambda^2 \omega_\lambda^2 Z_{\text{SQUID}}^2 (-\omega^2/2) h_0 \xi}{(i\omega)^2 + \tau_\lambda^{-1} i\omega + \omega_\lambda^2} \tag{1}$$

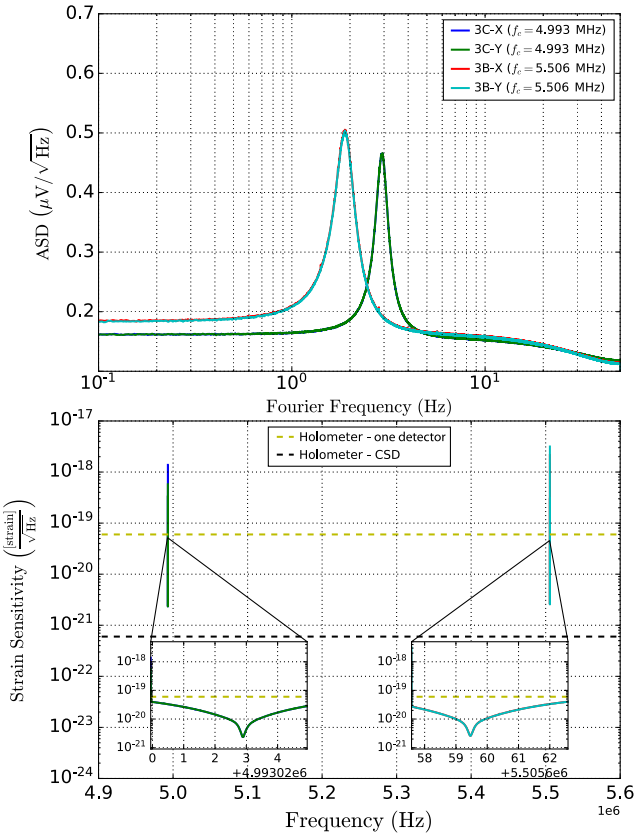

FIG. 3. Top figure displays averaged amplitude spectral density (ASD) of each output channel of lock-ins for longest continuous data taking run; here, each mode has been demodulated from the carrier. Bottom figure shows corresponding spectral strain sensitivity determined for each trace, as well as current best sensitivity in region given by Holometer experiment [6], which uses the cross spectral density (CSD) of two identical interferometers to search for HFGWs.

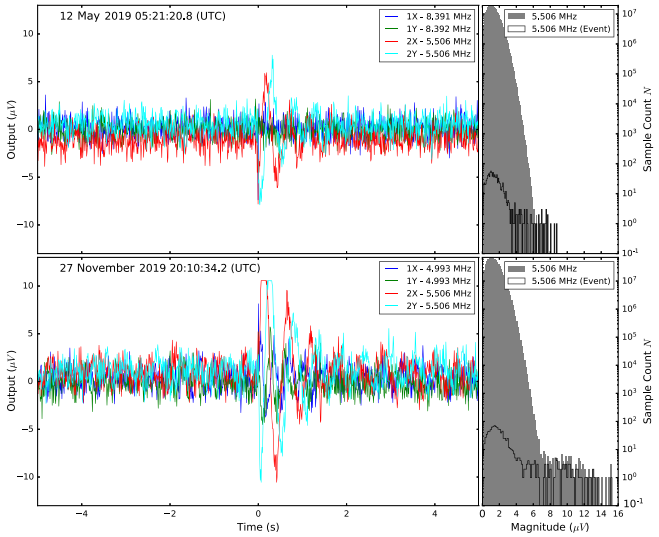

FIG. 4. Time series traces for two event signals detected by system. Each plot shows two quadratures for each mode. Also shown are histograms of output magnitude samples from only the 3B mode from both the entire corresponding run (gray) and just 10 s of data around the event (black). It is clear from this plot that the overwhelming majority of non-Gaussian outliers is due to these signals.

where Z_{SQUID} is the SQUID transimpedance, κ_λ is an experimentally found electromechanical coupling constant that relates charge on the BAW electrodes to displacement of the crystal [13], ω_λ is the mode frequency with mode decay time τ_λ, h_0 is the crystal thickness, and ξ is the weighting matrix term that parametrizes the coupling of the BAW to gravitational waves; it depends heavily on the effectiveness of phonon trapping in the acoustic modes.

Comparing our system to the only other HFGW detector in this frequency range, which is Fermilab's Holometer interferometer [6] (which provided spectral strain measurements from 1 to 13 MHz with 130 h of data collection), we see that we are within two orders of magnitude of the sensitivity given by the cross spectral density of their two 39 m long interferometers. With future generations of the quartz-based detector, we will be able to further increase sensitivity by using modes of a higher quality factor and explore higher frequencies without voiding the long wavelength approximation that limits larger scale detectors. It is also of note that the reported Holometer results were not sensitive to fast transient signals, such as the events we present here.

The total observation time for runs 1 and 2 was 3672.3 h, or 153 days. During this observation time, only two strongly significant events were detected: one for run 1 (12 March 2019 at 13:21:20.8 Australian western standard time), and one for run 2 (28 November 2019 at 04:10:34.2 Australian western standard time). Signal traces of these events are shown in Fig. 4, where each plot shows all four data channels (two quadratures of the two modes). Event 1 happens 5503 min after the start of the corresponding data acquisition, whereas event 2 happens 2247 min after; no other acquisition periods displayed events in these time ranges. Each event was a transient ring down with a measured decay constant of ≈1–2 s, which is consistent with the known quality factors of the BAW cavity modes. Thus, these events were most likely to have originated from within the BAW cavity and not any other part of the detection chain. The interaction itself would be well described by a single short pulse energy deposit in an acoustic mode. By calculating the kinetic energy of the resonating crystal, we estimate the energy deposition of events 1 and 2 to be of the order of $\approx 10\ \mu$eV.

It can be noted that event 1 was visible only for the 3B mode, whereas the 5C mode stays unperturbed at this level of sensitivity. The frequency difference between these modes was approximately 2.886 MHz. For event 2, the strongest signal was again produced for the 3B mode while still visible on the 3C modes. These modes were separated only by 513 kHz. In the second case, the modes were not

only closer in frequency but also of the same mode order (three variations of the acoustic field in the thickness). This might suggest that the experiment displays either frequency or mode order sensitivity to these events, in the process of detection. Additionally, mode polarization may have some effect on the signal shape in certain modes because slow and fast shear modes are almost (but not completely) mutually orthogonal with respect to the orientation of mechanical displacement relative to the direction of wave propagation.

We have compared timings of the observed events against other known observations of various nature available to the authors: (1) *Weather perturbations* (thunder in particular) may cause various disturbances to electrical circuits. Such events were ruled out based on the fact that corresponding time traces do not demonstrate any relation to acoustic resonances of the crystal. In any case, both events correspond to very calm days: the day of event 1 was sunny with a 31 °C temperature and 18 km/h wind, the night of event 2 was clear with $13-18$ °C temperatures and 21 km/h wind. (2) *Earthquakes* are known sources of acoustical vibration. However, the corresponding vibrational frequencies are much lower than the device's sensitive frequency region. Moreover, the BAW cavity was extremely well isolated from the ambient acoustic environment. No earthquakes in Australia were reported for the times of the events [30]. (3) The LIGO/VIRGO Collaboration reported no events on the corresponding days [31]. (4) The fourth possibility includes *meteor events and cosmic showers.* To the authors' knowledge, no documented meteor events or cosmic showers have occurred in the experiments location during the requisite time periods. (5) No documented *fast radio burst* events were detected in time near the events described in this work [32]. (6) The *Acoustic Lorentz Invariance Experiment* [33,34] is a sister experiment running to detect Lorentz invariance in the matter sector using quartz BAW oscillators working at 5 MHz in the same basement of the building (around 50 m away). No signals at the same times as the observed events were detected by this experiment.

Despite assigning the observed events to the BAW cavity itself rather than to the detection system, we do not claim that they were HFGWs of any source. In fact, there is a number of physical phenomena that can produce these kinds of events, ranging from internal solid state processes to highly speculative models of new physics. Here, we list some of the possibilities: (1) The first possibility includes an *internal solid state process* and stress relaxations of the quartz plate. Although quartz resonators exhibit various complex nonlinear phenomena, they have been observed at temperatures of a few millikelvins and subject to strong excitations [35,36]. In the current work, the detector was not connected to any electrical excitation circuit with the device terminals connected to the SQUID amplifier only. Although stress relaxation is a plausible explanation, the fact that some events have impact only on shear modes suggests that the stress is distributed in plane. (2) The second possibility includes *internal radioactive events.* It is known that the behaviours of acoustic devices can be altered when they are subject to ionising radiation [37,38]. These studies concern cumulative effects of radiation exposure for various applications. To the best of the authors' knowledge, no individual ionizing radiation events has been observed. (3) *Cosmic rays events* have been observed and detected by the previous generation of GW bar detectors working in a frequency range of a few hundred hertz [39,40]. For example, predicted cosmic ray event rates for NAUTILUS go as high as 107 events per day for 44.5 GeV of energy deposited into the detector, with the highest recorded event being 87 TeV and a range of other events spanning 0.04–57 K (where energy is given in units of kelvins). Because the BAW detector has an $\approx 10^4$ times smaller cross section, we would expect a reduction of events per day for a given energy of the same order when comparing to those seen in NAUTILUS. For the low energies, we have observed ($\lessapprox 20$ meV), and NAUTILUS would expect $> 10^6$ events per day; however, it is highly uncertain what fraction of the incident cosmic ray's energy would actually be deposited into the quartz. In future generations of this detector, cosmic ray events of this kind could be easily identified by employing muon (cosmic shower) detectors for coincidence analysis. (4) The fourth possibility includes *fireballs* and other meteor type events in the atmosphere [41,42]. The detector used in this work should not be sensitive to atmospheric acoustic waves because it was shielded by two layers of vacuum. Furthermore, excitation through the support structure was negligible because the vibrating part of the detector crystal was isolated from the support by etched gaps and a trapping mechanism. Finally, the sensitive frequency range was far from the typical acoustic frequencies of such events. (5) *HFGW sources* [2] were the premier targets of the experiment. Comparing to GWs detected by low frequency interferometric detectors, the observed events do not appear to represent mergers of any kind due to the lack of a chirp shape; however, due to the narrow-band nature of the detector, a merger event may still have been sampled to produce the observed impulse decay signal. The data best fit a single energy depositing event. Solving the detector equation of motion to match the strongest observed signal (event 2) results in a required characteristic strain amplitude of $h_c \approx 2.5 \times 10^{-16}$ if we assume the detector is excited by a transient $\tau_{\mathrm{GW}} = 1$ ms pulse of GW radiation. Such radiation could be explained by a primordial black hole merger of $m_{\mathrm{PBH}} < 4 \times 10^{-4} M_{\odot}$ (which gives a maximum frequency at an inspiral of 5.5 MHz) at a distance of $D \approx 0.01$ pc [2]. Additionally, rapid frequency evolution of the signal due to a short coalescence time would explain signal detection in two modes separated by ≈ 500 kHz. This discussion of possible HFGW sources is far from

exhaustive; many other models such as black hole superradiance and exotic compact object collisions can be tested, whereas analysis of low nontransient slow signals could also be achieved using existing data. Further HFGW analysis and discussions will be presented in a follow-up work, including future observational runs. (6) The sixth possibility includes *domain walls*, topological defects in dark matter, etc. Although these manifestations of dark matter are proposed to be detected with a network of magnetometers [43], it is quite viable that similar disturbances caused by topological defects in dark matter have mechanical manifestations detectable with the considered detector. This possibility has to be analyzed further. (7) *Weakly interactive massive particles* (WIMPs) [44], which are additional candidates for dark matter, are able to deposit energy in the form of phonons in crystals. Many WIMP detectors are, in fact, cryogenically cooled high purity crystals equipped with highly sensitive superconducting phonon detectors [45,46]. (8) The eighth possibility includes other types of *dark matter*, including composite candidates capable of producing single events in mechanical oscillators or phonons in crystals. (9) *Axion quark nuggets* [47] are claimed to be able to produce seismic and acoustic waves in a planet's atmosphere [48]; and they explain other anomalies such as a sun's corona anomaly [49] and DAMA/LIBRA results [50], as well as others. The axion quark nugget events described in the work with the alleged detection [48] can be ruled out based on the same points as for atmospheric meteor events.

In conclusion, we present the observation of rare events detected with a HFGW BAW cavity detector. At this point, no certain claim could be made on the origins of these events. The second implementation of this detector should rule out most of the possibilities. For this, the second generation detector will consist of two detector crystals with independent SQUID and digitizer readouts. In addition, the system will be equipped with a complementary muon detector to run a coincidence analysis with cosmic rays.

This research was supported by the Australian Research Council (ARC) Grant No. DP190100071, along with support from the ARC Centre of Excellence for Engineered Quantum Systems (No. CE170100009) and the ARC Centre of Excellence for Dark Matter Particle Physics (No. CE200100008).

*michael.tobar@uwa.edu.au

[1] B. P. Abbott *et al.* (LIGO Scientific and Virgo Collaborations), Phys. Rev. Lett. **116**, 061102 (2016).
[2] N. Aggarwal *et al.*, arXiv:2011.12414.
[3] T. Akutsu, S. Kawamura, A. Nishizawa, K. Arai, K. Yamamoto, D. Tatsumi, S. Nagano, E. Nishida, T. Chiba, R. Takahashi, N. Sugiyama, M. Fukushima, T. Yamazaki, and M.-K. Fujimoto, Phys. Rev. Lett. **101**, 101101 (2008).
[4] A. Nishizawa, S. Kawamura, T. Akutsu, K. Arai, K. Yamamoto, D. Tatsumi, E. Nishida, M.-a. Sakagami, T. Chiba, R. Takahashi, and N. Sugiyama, Phys. Rev. D **77**, 022002 (2008).
[5] A. M. Cruise, Classical Quantum Gravity **29**, 095003 (2012).
[6] A. S. Chou, R. Gustafson, C. Hogan, B. Kamai, O. Kwon, R. Lanza, S. L. Larson, L. McCuller, S. S. Meyer, J. Richardson, C. Stoughton, R. Tomlin, and R. Weiss (Holometer Collaboration), Phys. Rev. D **95**, 063002 (2017).
[7] C. Caprini and D. G. Figueroa, Classical Quantum Gravity **35**, 163001 (2018).
[8] J. G. C. Martinez and B. Kamai, Classical Quantum Gravity **37**, 205006 (2020).
[9] A. Ito, T. Ikeda, K. Miuchi, and J. Soda, Eur. Phys. J. C **80**, 179 (2020).
[10] N. Herman, A. Füzfa, S. Clesse, and L. Lehoucq, Phys. Rev. D **104**, 023524 (2021).
[11] T. Fujita, K. Kamada, and Y. Nakai, Phys. Rev. D **102**, 103501 (2020).
[12] V. Domcke and C. Garcia-Cely, Phys. Rev. Lett. **126**, 021104 (2021).
[13] M. Goryachev and M. E. Tobar, Phys. Rev. D **90**, 102005 (2014).
[14] P. Astone *et al.* (International Gravitational Event Collaboration), Phys. Rev. D **68**, 022001 (2003).
[15] D. G. Blair, E. N. Ivanov, M. E. Tobar, P. J. Turner, F. van Kann, and I. S. Heng, Phys. Rev. Lett. **74**, 1908 (1995).
[16] E. Mauceli, Z. K. Geng, W. O. Hamilton, W. W. Johnson, S. Merkowitz, A. Morse, B. Price, and N. Solomonson, Phys. Rev. D **54**, 1264 (1996).
[17] W. W. Johnson and S. M. Merkowitz, Phys. Rev. Lett. **70**, 2367 (1993).
[18] G. M. Harry, T. R. Stevenson, and H. J. Paik, Phys. Rev. D **54**, 2409 (1996).
[19] L. Baggio, M. Bignotto, M. Bonaldi, M. Cerdonio, L. Conti, P. Falferi, N. Liguori, A. Marin, R. Mezzena, A. Ortolan, S. Poggi, G. A. Prodi, F. Salemi, G. Soranzo, L. Taffarello, G. Vedovato, A. Vinante, S. Vitale, and J. P. Zendri, Phys. Rev. Lett. **94**, 241101 (2005).
[20] O. D. Aguiar *et al.*, Classical Quantum Gravity **25**, 114042 (2008).
[21] A. Arvanitaki and A. A. Geraci, Phys. Rev. Lett. **110**, 071105 (2013).
[22] N. Aggarwal, G. P. Winstone, M. Teo, M. Baryakhtar, S. L. Larson, V. Kalogera, and A. A. Geraci, arXiv:2010.13157.
[23] S. Galliou, M. Goryachev, R. Bourquin, P. Abbe, J. Aubry, and M. Tobar, Nature (London) **3**, 2132 (2013).
[24] M. Goryachev, D. L. Creedon, E. N. Ivanov, S. Galliou, R. Bourquin, and M. E. Tobar, Appl. Phys. Lett. **100**, 243504 (2012).
[25] D. Stevens and H. Tiersten, J. Acoust. Soc. Am. **79**, 1811 (1986).
[26] R. J. Besson, in *Proceedings of the 31st Annual Symposium on Frequency Control* (IEEE, Atlantic City, 1977), p. 147.
[27] ANSI/IEEE Std 176-1987, IEEE Standard on Piezoelectricity, IEEE 176-1987 (1988), https://doi.org/10.1109/IEEESTD.1988.79638.
[28] S. Galliou, M. Goryachev, R. Bourquin, P. Abbé, J. P. Aubry, and M. E. Tobar, Sci. Rep. **3**, 2132 (2013).

[29] M. Goryachev, E. N. Ivanov, F. van Kann, S. Galliou, and M. E. Tobar, Appl. Phys. Lett. **105**, 153505 (2014).
[30] Geoscience Australia, https://earthquakes.ga.gov.au.
[31] GraceDB, https://gracedb.ligo.org/latest/.
[32] F. list, http://frbcat.org.
[33] M. Goryachev, Z. Kuang, E. N. Ivanov, P. Haslinger, H. Müller, and M. E. Tobar, IEEE Trans. Ultrason. Ferroelectr. Freq. Control **65**, 991 (2018).
[34] A. Lo, P. Haslinger, E. Mizrachi, L. Anderegg, H. Müller, M. Hohensee, M. Goryachev, and M. E. Tobar, Phys. Rev. X **6**, 011018 (2016).
[35] M. Goryachev, W. G. Farr, S. Galliou, and M. E. Tobar, Appl. Phys. Lett. **105**, 063501 (2014).
[36] M. Goryachev, S. Galliou, and M. E. Tobar, Phys. Rev. Research **2**, 023035 (2020).
[37] J. Friedt, C. Mavon, S. Ballandras, V. Blondeau-Patissier, and M. Fromm, in *Proceedings of the 8th European Conference on Radiation and Its Effects on Components and Systems, 2005* (IEEE, Cap d'Agde, 2005), p. PI3–1.
[38] J. Lefèvre, S. Devautour-Vinot, O. Cambon, J. J. Boy, P. Guibert, R. Chapoulie, C. Inguimbert, D. Picchedda, A. Largeteau, G. Demazeau, and G. Cibiel, J. Appl. Phys. **105**, 113523 (2009).
[39] P. Astone *et al.*, Phys. Lett. B **499**, 16 (2001).
[40] P. Astone, D. Babusci, M. Bassan, P. Bonifazi, G. Cavallari, E. Coccia, S. Dantonio, V. Fafone, G. Giordano, and C. Ligi, Astropart. Phys. **30**, 200 (2008).
[41] R. Spalding, J. Tencer, W. Sweatt, B. Conley, R. Hogan, M. Bosslough, G. Gonzales, and P. Spurný, Sci. Rep. **7**, 41251 (2017).
[42] A. E. Dudorov and O. V. Eretnova, Solar System Research **54**, 223 (2020).
[43] M. Pospelov, S. Pustelny, M. P. Ledbetter, D. F. J. Kimball, W. Gawlik, and D. Budker, Phys. Rev. Lett. **110**, 021803 (2013).
[44] G. Jungman, M. Kamionkowski, and K. Griest, Phys. Rep. **267**, 195 (1996).
[45] G. Angloher *et al.*, Phys. Rev. Lett. **117**, 021303 (2016).
[46] A. Juillard, J. Low Temp. Phys. **151**, 806 (2008).
[47] S. Ge, K. Lawson, and A. Zhitnitsky, Phys. Rev. D **99**, 116017 (2019).
[48] D. Budker, V. Flambaum, and A. Zhitnitsky, arXiv:2003.07363v2.
[49] N. Raza, L. Van Waerbeke, and A. Zhitnitsky, Phys. Rev. D **98**, 103527 (2018).
[50] A. Zhitnitsky, Phys. Rev. D **101**, 083020 (2020).